Published in final edited form as:
Biofabrication. 2012 September ; 4(3): 035003. doi:10.1088/1758-5082/4/3/035003.

An automated two-phase system for hydrogel microbead production

Daniela F. Coutinho[1,2,3,4,□], **Amir F. Ahari**[3,4,□], **Nezamoddin N. Kachouie**[3,4,□], **Manuela E. Gomes**[1,2], **Nuno M. Neves**[1,2], **Rui L. Reis**[1,2], and **Ali Khademhosseini**[3,4,5,*]

[1]3B's Research Group – Biomaterials, Biodegradables and Biomimetics, Dept. of Polymer Engineering, University of Minho, Headquarters of the European Institute of Excellence on Tissue Engineering and Regenerative Medicine, AvePark, Taipas, 4806-909 Guimarães, Portugal

[2]ICVS/3B's - PT Government Associate Laboratory, Braga/Guimarães, Portugal

[3]Center for Biomedical Engineering, Department of Medicine, Brigham and Women's Hospital, Harvard Medical School, Cambridge, MA 02139, USA

[4]Harvard-MIT Division of Health Sciences and Technology, Massachusetts Institute of Technology, Cambridge, MA 02139, USA

[5]Wyss Institute for Biologically Inspired Engineering, Harvard University, Boston, MA 02115, USA

Abstract

Polymeric beads have been used for protection and delivery of bioactive materials, such as drugs and cells, for different biomedical applications. Here we present a generic two-phase system for the production of polymeric microbeads of gellan gum (GG) or alginate (ALG), based on a combination of *in situ* polymerization and phase separation. Polymer droplets, dispensed using a syringe pump, formed polymeric microbeads while passing through a hydrophobic phase. These were then crosslinked, and thus stabilized, in a hydrophilic phase as they crossed through the hydrophobic-hydrophilic interface. The system can be adapted to different applications by replacing the bioactive material and the hydrophobic and/or the hydrophilic phases. The size of the microbeads was dependent on the system parameters, such as needle size and solution flow rate. The size and morphology of the microbeads produced by the proposed system were uniform, when parameters were kept constant. This system was successfully used for generating polymeric microbeads with encapsulated fluorescent beads, cell suspensions and cell aggregates proving its ability for generating bioactive carriers that can potentially be used for drug delivery and cell therapy.

Keywords

Bead Formation; Encapsulation; Automated System; Ionic Polymers; Gellan Gum

[*]Corresponding author (Prof. A. Khademhosseini). alik@rics.bwh.harvard.edu.
[□]These authors contributed equally.

Author Contribution

DFC, AFA, NNK and AK designed the study; DFC, AFA, NNK performed the experiments; DFC, AFA, NNK and AK wrote the paper. MG, NN, RR revised the paper. All authors discussed the results and commented on the manuscript.

1. Introduction

Current therapeutic products often rely on the systemic injection of high doses of bioactive materials that may trigger an autoimmune response or cause other adverse effects in the human body. Encapsulation of bioactive entities within immune-protective systems is an effective way to overcome these challenges. Microencapsulation of bioactive agents, such as drugs [1], enzymes [2, 3], cell suspensions [4–6], or cell aggregates [7, 8], has provided promising therapeutics for different diseases such as diabetes [9], hemophilia [10], and cancer [11, 12] and holds the potential to significantly improve the efficacy in the treatment of a variety of other clinical settings, such as engineering heart tissue grafts [13].

Many polymers have been proposed for the development of micro and nanobeads, such as poly(hydroxyethyl methacrylate-co-methyl methacrylate) [5, 14], poly(lactic-co-glycolic) acid [15, 16], chitosan [17], carrageenan [18], alginate (ALG) [19, 20], and gellan gum (GG) [21, 22]. The protective biocompatible polymeric outer layer of the bead is the primary surface to interact with the host immune system once implanted. This indirect contact of the bioactive agent with the human body significantly decreases the risk of immune-rejection and maximizes the availability of the bioactive entity at the target tissue. Thus, the selection of the appropriate polymer for a specific therapy is of key importance and depends on different factors, namely the encapsulated bioactive material and the therapeutic target. Specifically, GG has been reported to successfully incorporate in microbeads different drugs, such as cephalexin [23] or glipizide [24] as well as to viably encapsulate various types of cells, both from bacterial [25] and animal [22] sources. In fact, several clinical trials have demonstrated the viability and functionality of encapsulated cells [26, 27], motivating researchers to develop novel microencapsulation techniques with improved performance.

Several methods have been proposed to tailor the bead size, morphology, and encapsulation efficiency for different applications [28–31]. The major challenges that must be addressed by new microbead production systems are: (i) uniform bead fabrication, (ii) maintenance of the bioactivity of the encapsulated material throughout the process, and (iii) possibility to fabricate microbeads with different sizes, depending on the application. Various encapsulation techniques have been proposed for the development of polymeric beads, including those based in principles of electrostatic polymer interactions [19], phase separation [32] and *in situ* polymerization [33]. Polymerizing *in situ* ionotropic polymers with divalent ions (such as Ca_2^+) is one of the most widely reported encapsulation methods [33–35]. However, in some cases, when the polymer droplet first contacts the crosslinking solution, polymer beads with an inconsistent shape may be developed. The fabrication of microbeads with improved shape has been reported by combining a phase separation process with this *in situ* polymerization of the polymeric beads. Sefton MV and colleagues have described a system that uses a liquid-liquid two-phase system for the production of hollow microcapsules . They reported the use of hexadecane as the hydrophobic phase used for microcapsule formation and phosphate buffer saline as the hydrophilic solution for *in situ* crosslinking of the polymer.

Herein, a new microbead production system is introduced to accomplish the microbead formation and stabilization in a single automated procedure. Our system combines the principles of hydrophobic-hydrophilic repulsion forces previously reported [14], with gravity and mechanical forces to develop polymeric beads of GG or ALG. The hydrophilic phase enabled the formation of the microbeads, which then passed through the liquid-liquid phase interface by gravity and by mechanical forces induced by a rocking platform shaker. The stabilization of the polymeric microbeads was achieved once they reached the hydrophilic phase. The system can be easily modified for different applications by replacing the bioactive material or the hydrophobic/hydrophilic solutions. Microbeads with uniform

shape, size, and morphology were successfully produced by the proposed system using GG or ALG, showing the wide applicability of the system.

2. Materials and Methods

2.1. Materials

The materials used in this study were gellan gum (GG, Gelrite®, Sigma-Aldrich) and alginic acid sodium salt (ALG, Sigma-Aldrich). The light mineral oil used was purchased from Sigma-Aldrich. 3 mL BD™syringes with tip cap, clear (100/sp, 500/ca) and needles (31 G × 1 1/2 in, 27 G × 1 1/2 in, 25 G × 1 1/2 in gauge) were purchased from BD Biosciences. Fluoresbrite® Yellow Green fluorescent polystyrene latex microspheres (10.0 μm) packaged as 2.5% aqueous suspension with 4.55×10^7 particles/mL were purchased from Polysciences (Warrington, PA). Calcium chloride ($CaCl_2$, M_w = 110.98 g/mol) was purchased from Sigma-Aldrich.

2.2. Preparation of solutions

GG solution was prepared as previously described [37]. Briefly, 1% (w/v) solution of GG was prepared by dissolving the powder in deionized water for 20–30 min at 90 °C and stabilized at 40 °C. Similarly, ALG solution was prepared at 1% (w/v) by dissolving 1 g of ALG in 100 mL Dulbecco's Phosphate Buffer Saline (DPBS, Sigma).

2.3. Microbead generation

Microbeads containing GG or ALG were produced in a single automated procedure, similar to a process described before [14]. The schematic of the automated microbead production system is depicted in figure 1 (setup shown in figure A1). Briefly, the system contains three main units: a controllable syringe pump device, a laboratory shaker and a container filled with a hydrophilic and a hydrophobic solution. The syringe pump (New Era Pump Systems, NE-300, USA) was placed vertically and a 3 mL syringe loaded. The parameters of the rocking platform shaker (VWR, 12620-906, USA) were set to: speed of 32 rpm and tilt angle from 0° to 4°. The two-phase system, formed by two distinct phases in the container, was obtained by having mineral oil as the hydrophobic solution (with lower density, top) and cell culture medium (Dulbecco's Modified Eagle Medium, DMEM, Sigma-Aldrich) or $CaCl_2$ as the hydrophilic solution (higher density, down). Microbead formation was carried out by first dispensing polymeric droplets into the mineral oil using a syringe pump. Agitation produced by the rocking shaker was used to decrease the size of the microbeads produced, thus increasing the number of microbeads generated. Due to the hydrophobicity of the mineral oil, perfectly spherical microbeads were generated in this solution. When beads passed through the mineral oil-medium interface, they start to chemically crosslink by the crosslinking agent present in the hydrophilic solution. Specifically, GG and ALG were crosslinked by calcium ions contained in the medium and $CaCl_2$ solution, respectively. The beads suspended in the hydrophilic solution were directly stored in the incubator.

2.3.1. Microbead generation with encapsulated fluorescent beads—The possibility to uniformly encapsulate drug-like particles was evaluated using fluorescent beads. Stock solutions containing fluorescent microbeads with a diameter of 10.0 μm (with a solid fraction of 0.1% w/w) were suspended in the GG polymer solution at 37 °C. Two different bead concentrations, 0.01% (i.e., 4.55×10^5 beads/mL) and 0.1% (i.e., 4.55×10^6 beads/mL) of the original concentration (i.e., 4.55×10^7 beads/mL) were used to assess the influence of bead concentration over its distribution within the microgels. The process for generating encapsulated fluorescent beads was similar to that used for the simple microbeads. Encapsulated fluorescent beads were imaged using a fluorescence microscope.

2.3.2. Microbead generation with encapsulated NIH-3T3 cells—NIH-3T3 fibroblast cells were cultured in Dulbecco's Modified Eagle Medium (DMEM, Sigma-Aldrich) supplemented with heat-inactivated fetal bovine serum (10%, FBS, Gibco) and penicillin-streptomycin (1%, Gibco) at 37 °C, in a humidified atmosphere with 5% of CO_2. A cell suspension (3×10^6 cells/mL) was prepared by trypsinizing NIH-3T3 cells with trypsin/EDTA solution (Gibco) and mixing the cell suspension with the GG polymer solution at 37 °C. The process for generating beads with NIH-3T3 cells was similar to that used for the simple microbeads. The viability of the encapsulated cells in the hydrogels was characterized 1, 3, 5 and 7 days after culture, by incubating cells with a Live/Dead assay (calcein AM/ethidium homodimer-1, Invitrogen) during 20 min.

2.3.3. Microbead generation with encapsulated MIN6 cell aggregates—A murine insulinoma cell line (MIN6) was kindly provided by Dr. Donald Ingber, Wyss Institute of Harvard, Boston, MA, USA. MIN6 cells (passages 35– 42) were maintained at 37 °C and 5% CO_2 in DMEM supplemented with 10% FBS, 100 U/mL penicillin and 0.1 mg/mL streptomycin. The medium was changed every 3–4 days and cultured cells were used for MIN6 pseudo-islet formation when reaching 70% confluence. MIN6 pseudo-islets were formed by seeding MIN6 cells with 6×10^6 cells/mL concentration in poly(ethylene glycol) (PEG) microwells with a diameter of 300 μm for 3 days (figure A2). The MIN6 aggregates were harvested and preserved in medium immediately before encapsulation. MIN6 cell aggregates were suspended in GG polymer solution at 37 °C and transferred to a 3 mL syringe for dispensing and microencapsulation. MIN6-GG suspension was dispensed into the two-phase system (mineral oil-cell culture medium) and encapsulated pseudo-islets were formed. Immunofluorescence was used to assess the expression of insulin by encapsulated islets. Anti-Insulin receptor substrate 2 antibody produced in rabbit (Sigma-Aldrich) was coupled with a secondary antibody AlexaFluor 546-conjugated anti-rabbit (Sigma-Aldrich) in order to detect fluorescence.

2.4. Microbead characterization

To characterize the influence of the system parameters over the size of the microbeads, the needle gauge (connected to the syringe) and the flow rate at which the polymer was dispensed were varied. Thus, the flow rate of the solution was set to 0.01 μL/min and the needle gauge varied from 31 to 27 and 25G. On the other hand, with a needle gauge of 31G, three values of flow rate of the polymer solution were tested: 0.002, 0.01 and 0.1 μL/min. The influence of the flow rate and the needle size over the microbead size was evaluated by examining the diameter of 30 distinct beads under a standard inverted-light microscope. The size of the beads was measured using ImageJ software (http://rsbweb.nih.gov/ij/) by measuring the diameter of a circle drawn over the edge of the microbead. The shape of the beads was assessed by measuring the aspect ratio of the beads (major axis:minor axis). Other parameters of the system were kept fixed throughout all of the experiments including the speed and the tilt angle of the rocking platform shaker and the syringe volume (3 mL). The reproducibility of the system was evaluated by measuring the microbead size (three independent experiments, each containing at least 15 microbeads) and shape (n=12). . In addition to GG microbeads, ALG microbeads were also produced to evaluate the possibility of engineering microbeads of other polymers using the described system.

2.5. Statistical analysis

Data were subjected to statistical analysis and reported as mean ± standard deviation. Analysis of variance (One-Way, $p<0.05$, and Two-Way ANOVA, $p<0.0001$) was used for statistical analysis.

3. Results and Discussion

3.1. Size-controlled microbead formation

Beads with uniform sizes and shapes have been made at the macro-level and have found several clinical and pharmaceutical applications [7, 12, 34]. Specifically, GG microbeads with 1–2 mm in diameter have been produced, mainly using *in situ* precipitation methodologies [23, 24, 38]. However, the delivery of microbeads with encapsulated bioactive materials including drugs, cell suspensions and cell aggregates to the patient might require a smaller scale. Moreover, it is a challenge to obtain GG microbeads with uniform size and shape with the current methologies. Thus, there is a demand for the development of an automated system with capability of continuous microbead production without manual intervention. Even more important is the need of a system that can be easily tuned according to the encapsulated biological entity and therefore to the therapeutic application. Herein, we have addressed the issue of automated production of GG microbeads by means of a liquid-liquid two phase system, as shown in figure 1.

In previous works [14, 39], polymeric microbeads were formed in a hydrophobic solution where oil was employed as a sheath fluid. Furthermore, Sefton and colleagues have described a process for the development of hollow microcapsules using a coaxial system in which cells and the polymer solution were extruded through different barrels. The formed microcapsules passed through a hexadecane solution and were collected in a PBS curing bath. Hollow microcapsules were produced and the cell suspension incorporated in the interior of the microcapsule. In our system, mineral oil was the selected hydrophobic phase and culture medium the hydrophilic phase used to crosslink GG polymer. For the production of ALG beads, used to show the versatility of the system, $CaCl_2$ was used as the reticulating agent. Aiming at using this system for different biomedical applications, it is highly desired that the final step of bead production (stabilization) occurs in a biocompatible hydrophilic solution. As illustrated in figure 1, GG polymeric droplets passed through a hydrophobic material (mineral oil) and polymerized in a hydrophilic solution (culture medium). Briefly, the syringe pump flowed the polymer solution, forming polymer droplets at the tip of the syringe needle. As the increasing polymer mass met the mineral oil, the forces of gravity and surface tension between the polymer and the mineral oil pulled the polymer droplet into the hydrophobic phase, forming a microbead. Once it passed through the liquid-liquid two-phase interface, they started to crosslink, and thus to stabilize, by the action of the Ca^{2+} ions present in the hydrophilic phase. In contrast to what was observed in previous works [14, 36], the polymerization of encapsulated cells in cell culture medium allows for minimal manual manipulation since it is not required to harvest the beads before cell culture. This feature not only contributes to the formation of damage-free beads but also, indirectly contribute to the protection of the biofunctionality of the encapsulated bioactive materials. The effective stabilization of the GG microbeads was confirmed by their non-aggregation when kept in cell culture medium. The viability and functionality of the encapsulated cell suspension and cell aggregates were investigated and are described in detail in the following sections.

3.1.1. Influence of system parameters over size of microbeads—The size of microbeads can be mainly controlled by the needle size, flow rate of the polymeric solution, viscosity of the hydrophobic phase and tilt and speed of the rocking platform shaker. During the optimization process, it was found that the size of the microbeads was dependent on the needle size and flow rate of the polymeric solution. It was also found that a hydrophobic phase with high viscosity would hamper the production of the beads. Thus, mineral oil with low viscosity was selected. Moreover, the tilt and speed of the rocking platform shaker were found to play a role on facilitating and controlling the speed of the bead production and size

uniformity. Therefore, the needle size and the flow rate of the polymer solution were varied, while the other parameters were kept constant (figure 2). As the polymer solution was pumped with a specific rate through the needle, the polymer mass on the needle tip was stretched, forming polymeric droplets. Beads were formed in the hydrophilic phase through the combination of four main forces: polymer-needle surface tension, polymer-mineral oil interfacial tension, mineral oil-cell culture medium interfacial tension and gravity (figure 2D).

To analyze the effect of polymer solution dispensing rate over the bead size, the needle size was fixed to 31G (approximately 135 μm of inner diameter) and the fluid flow rate was set to 0.002, 0.01 or 0.1 μL/min. As depicted in figure 2A, the diameter of the microbeads significantly increased (One-way Anova, $p<0.05$) from 270 to 340, and to 480 μm with increasing fluid flow rates. This might be a result of a specific combination of the forces involved in the process. As the shaker tilted, the mineral oil periodically met the stretched polymer on the needle tip. As the combination of gravity and polymer-mineral oil interfacial tension forces dominated the polymer-needle surface tension, the polymer droplet separated from the needle tip, forming the microbead. For higher pump rates, the volume of polymer dispensed for a given period of time (the time the shaker takes to move from 4° to 0°) was higher, leading to the formation of larger microbeads.

The influence of needle diameter over the size of the produced microbeads (figure 2B) was also investigated by fixing the pump rate at 0.01 μL/min and varying the size of the needle (31, 27 and 25 G). It was observed that microbeads showed increasing average size of 340, 400 and 600 μm, with increasing diameter of the needle, being significantly different between each other (One-way Anova, $p<0.05$). With a larger needle gauge, the polymer-needle surface tension is stronger, which is directly related to the higher surface area of the needle tip. As a result, stronger forces (gravity combined with polymer-mineral oil interfacial tension) are needed to separate the higher mass of stretched polymer solution from the needle tip. Regardless of the needle size used, the microbead diameter was greater than the diameter of the needle tip.

3.1.2. Versatility of the system and applicability to different polymeric materials—To investigate the versatility of the proposed system, we have analyzed the influence of the pump rate of the polymer solution over the microbead size using another well studied polymer in tissue engineering. ALG has been widely used in encapsulation systems due to its easy manipulation [20, 34]. Similarly to the findings for GG, figure 2C demonstrates that the size of the microbeads of ALG was dependent on the pump rate, significantly increasing (One-way Anova, $p<0.05$) as the pump rate increases. Interestingly, the diameter of the ALG microbeads was significantly smaller (Two-way Anova, $p<0.0001$) than the one registered for the GG microbeads. This might be a result of the different properties of the polymers used, namely the viscosity and surface tension.

3.1.3. Reproducibility of the system—To investigate the reproducibility and uniformity of the produced microbeads by controlling either the pump rate or the needle size, experiments were repeated three times (figure 3A,B,C) for each condition (n=15). The size uniformity of generated GG and ALG microbeads can be easily observed for both parameters. Also, the frequency distribution of the diameter of the produced microbeads was analyzed for the three needle sizes (figure 3D,E,F). A relative increased polydispersity was observed with increasing needle gauge. The uniformity of the shape of the beads produced was evaluated by measuring the aspect ratio (major axis of the bead over the minor axis of the bead) for all the parameters tested (Figure 3G,H). Beads with uniform shape were produced with all needle sizes tested. Nevertheless, a decrease on shape uniformity of the beads for the highest flow rate tested (0.1 μL/min) was observed. These results demonstrated

a precise control over the microbead size and shape in the proposed system for the production of polymeric microbeads in three distinct experiments performed.

3.2. System Applications

Different types of polymers, including synthetic and natural polymers, have been used with considerable success for cell encapsulation. Herein, the production of micro-scaled GG microbeads was aimed. GG has shown promising results both *in vitro* and *in vivo* as a scaffold for cartilage tissue engineering [22, 40]. The divalent (Ca^{2+}, Mg^{2+}) and monovalent (Na^{+}, K^{+}) cations in the cell culture medium, which was used as the hydrophilic phase in the proposed liquid-liquid two-phase system for cell suspension and cell aggregate encapsulation, were sufficient for crosslinking this ionic polymer. For non-cell based beads, including controlled release of drugs, culture medium can be replaced by other ionic hydrophilic solutions such as PBS, which is also known to crosslink GG [37]. Ions could also be added to non-ionic hydrophilic solutions to optimize microbead stabilization.

The ability to quickly generate microbeads with different encapsulated bio-entities within the proposed system was explored and is depicted in figure 4. Our system was able to successfully encapsulate from simple microbeads to complex biological entities, such as functional cell aggregates. In the following sections, each application is described in detail.

3.2.1. Particle encapsulation—The proposed system can potentially be used for the incorporation of particles, such as drugs, being ultimately used as sustained drug release systems [41]. This application was investigated by encapsulating green fluorescent beads (10 μm in diameter) in GG microbeads by the proposed system. The developed GG microbeads were imaged immediately after microbead formation, as depicted in figure 4A. Two different concentrations of encapsulated microbeads were used (low and high) to evaluate the ability to homogenously encapsulate different drug concentrations. This procedure could be used for potentially encapsulating particles with different sizes, shapes and biofunctionality for drug delivery applications.

3.2.2. Viability of encapsulated cells—The proposed system is cell-compatible as harsh crosslinking processes such as UV and aggressive chemical crosslinking mechanisms are avoided. The viability of the encapsulated cells was investigated 1, 3, 5, and 7 days after culture, as depicted in figure 4B. NIH-3T3 fibroblast cells encapsulated within the microbeads were stained with calcein AM, which is well retained in living cells, producing an intense green fluorescence and with ethidium homodimer (EthD-1), which enters the damaged cell membrane (dead cell), binding to nucleic acids. As observed in figure 4B, most of the cells seem to be alive after 3 days of culture, indicating that the process of fabrication of the microbeads showed to have no significant effect on the viability of encapsulated cells. Nevertheless, lower cell viability at longer culture periods (day 5 and day 7) point towards a possible need of optimization of the polymeric system and its crosslinking mechanism. . The encapsulation of cell suspension using the proposed system allowed a good distribution of encapsulated NIH-3T3 cells within GG microbeads.

Moreover, this system enabled culturingcells in the medium immediately after their production without further washing, filtering, transferring or any other manipulation or intervention. This attractive attribute possibly contributed to an increase in cell viability.

3.2.3. Functionality of encapsulated cell aggregates—To investigate the ability to encapsulate functional aggregates of cells, aggregates of MIN6 cells were encapsulated in GG beads and insulin secretion detected by immunofluorescence. Initially, MIN6 cells were seeded in PEG-made microwells with 300 μm diameter and incubated in cell culture

medium for three days. The microwell fabrication and pseudo-islet production are explained in detail as supplementary data (figure A2). Cell aggregates were harvested on day three, mixed with the GG hydrogel solution and used to produce encapsulated pseudo-islets using the proposed system. As shown in figure 4C, cell aggregates were encapsulated in GG beads and their functionality was assessed by detecting insulin secretion through immunostaning. The red fluorescence present on the cell aggregates and not on the polymeric bead (figure 4C-iii) demonstrated that the encapsulated cell aggregates were secreting insulin. These results showed that the system allowed not only to produce microbeads with viable encapsulated cells, but also enabled the production of microbeads with cell aggregates that are able to maintain the ability to produce insulin.

4. Conclusions

We proposed a reproducible mechanism for the production of microbeads by using two distinct liquid phases. By means of a syringe pump, the polysaccharides GG or ALG were dispensed in the hydrophobic phase, leading to the formation of microbeads. Through the action of gravity and mechanical forces, the microbeads crossed the interface of the solutions, falling from the hydrophobic phase into the hydrophilic one. The crosslinking agent, present in the hydrophilic phase, allowed obtaining the stabilization of the microbeads. Encapsulated beads, cell suspensions and cell aggregates were successfully produced. By changing the hydrophobic and/or hydrophilic solution, this method can be applied to a broad range of microbead formulations. Our simple and functional system was successfully demonstrated by producing microbeads with different materials, uniform size and morphology in an automated system.

Acknowledgments

This research was funded by the US Army Engineer Research and Development Center, the Institute for Soldier Nanotechnology, the NIH (HL092836, EB007249), and the National Science Foundation CAREER award (AK). This work was partially supported by the Portuguese Foundation for Science and Technology (FCT), through funds from the POCTI, FEDER and MIT-Portugal (MIT/ECE/0047/2009) programs and from the European Union under the project NoE EXPERTISSUES (NMP3-CT-2004-500283). DFC acknowledges FCT and the MIT-Portugal Program for personal grant SFRH/BD/37156/2007.

Appendix

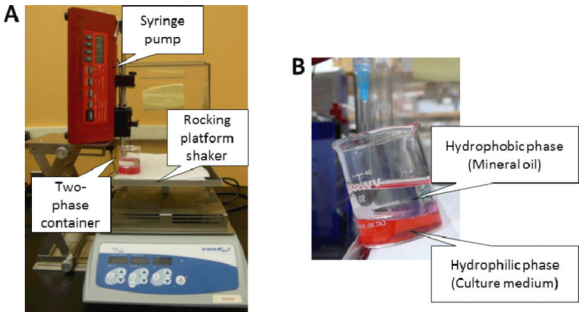

Figure A1. (A) Setup of the two-phase system with the syringe pump, two-phase container and rocking platform shaker depicted. (B) Amplified image of the two-phase container showing the hydrophobic and hydrophilic phases.

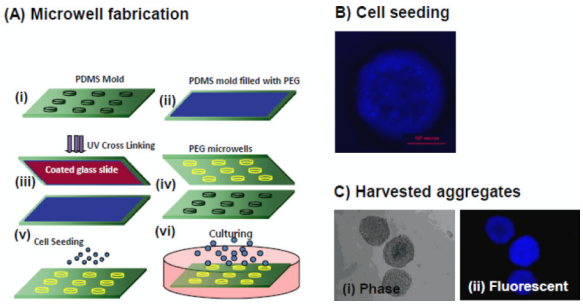

Figure A2. Preparation of cell aggregates: (A) microwell fabrication; (B) cell seeding and (C) harvested cell aggregates.

References

1. Cleland JL, Johnson OL, Putney S, Jones AJS. Recombinant human growth hormone poly(lactic-co-glycolic acid) microsphere formulation development. Adv Drug Deliv Rev. 1997; 28(1):71–84. [PubMed: 10837565]
2. Cadenazzi G, Streitenberger S, Cerone S, Sansinanea A. Immobilization of enzymes: Micro-encapsulation of Glutathione-S-transferase. Acta Bioquim Clin Latinoam. 2003; 37(4):401–404.
3. Lambert JM, Weinbreck F, Kleerebezem M. In vitro analysis of protection of the enzyme bile salt hydrolase against enteric conditions by whey protein-gum arabic microencapsulation. J Agric Food Chem. 2008; 56(18):8360–8364. [PubMed: 18729459]
4. Orive G, Hernandez RM, Gascon AR, Calafiore R, Chang TMS, Vos PD, Hortelano G, Hunkeler D, Lacik I, Shapiro AMJ, et al. Cell encapsulation: Promise and progress. Nat Med. 2003; 9(1):104–107. [PubMed: 12514721]
5. Boag AH, Sefton MV. Microencapsulation of human-fibroblasts in a water-insoluble polyacrylate. Biotechnol Bioeng. 1987; 30(8):954–962. [PubMed: 18581534]
6. McGuigan AP, Bruzewicz DA, Glavan A, Butte M, Whitesides GM. Cell Encapsulation in Sub-mm Sized Gel Modules Using Replica Molding. Plos One. 2008; 3(5)
7. Hasse C, Klock G, Schlosser A, Zimmermann U, Rothmund M. Parathyroid allotransplantation without immunosuppression. Lancet. 1997; 351:1296–1297. [PubMed: 9357413]
8. Soon-Shiong P. Insuline independence in a type-1 diabetic patient after encapsulated islet transplantation. Lancet. 1994; 343:950–951. [PubMed: 7909011]
9. Sun YL, Ma XJ, Zhou DB, Vacek I, Sun AM. Normalization of diabetes in spontaneously diabetic cynomologus monkeys by xenografts of microencapsulated porcine islets without immunosuppression. J Clin Invest. 1996; 98(6):1417–1422. [PubMed: 8823307]
10. Hortelano G, AlHendy A, Ofosu FA, Chang PL. Delivery of human factor IX in mice by encapsulated recombinant myoblasts: A novel approach towards allogeneic gene therapy of hemophilia B. Blood. 1996; 87(12):5095–5103. [PubMed: 8652822]
11. Xu WM, Liu LZ, Charles IG. Microencapsulated iNOS-expressing cells cause tumor suppression in mice. FASEB J. 2001; 15(14):213–215. [PubMed: 11772948]
12. Shi MQ, Hao S, Quereshi M, Guo WL, Zheng CY, Xiang J. Significant tumor regression induced by microencapsulation of recombinant tumor cells secreting fusion protein. Cancer Biother Radio. 2005; 20(3):260–266.
13. Bai XP, Zheng HX, Fang R, Wang TR, Hou XL, Li Y, Chen XB, Tian WM. Fabrication of engineered heart tissue grafts from alginate/collagen barium composite microbeads. Biomedical Materials. 2011; 6(4)
14. Sefton MV, Dawson RM, Broughton RL, Blysniuk J, Sugamori ME. Microencapsulation of mammalian-cells in a water-insoluble polyacrylate by coextrusion and interfacial precipitation. Biotechnol Bioeng. 1987; 29(9):1135–1143. [PubMed: 18576568]

15. Yin JH, Noda Y, Yotsuyanagi T. Properties of poly(lactic-co-glycolic acid) nanospheres containing protease inhibitors: Camostat mesilate and nafamostat mesilate. Int J Pharm. 2006; 314(1):46–55. [PubMed: 16551494]
16. Emami J, Hamishehkar H, Najafabadi AR, Gilani K, Minaiyan M, Mahdavi H, Nokhodchi A. A Novel Approach to Prepare Insulin-Loaded Poly (Lactic-Co-Glycolic Acid) Microcapsules and the Protein Stability Study. J Pharm Sci. 2009; 98(5):1712–1731. [PubMed: 18855911]
17. Taqieddin E, Amiji M. Enzyme immobilization in novel alginate-chitosan core-shell microcapsules. Biomaterials. 2004; 25(10):1937–1945. [PubMed: 14738858]
18. Grenha A, Gomes ME, Rodrigues M, Santo VE, Mano JF, Neves NM, Reis RL. Development of new chitosan/carrageenan nanoparticles for drug delivery applications. J Biomed Mater Res Part A. 2010; 92A(4):1265–1272.
19. van Hoogmoed CG, Busscher HJ, de Vos P. Fourier transform infrared spectroscopy studies of alginate-PLL capsules with varying compositions. J Biomed Mater Res Part A. 2003; 67A(1):172–178.
20. Koch S, Schwinger C, Kressler J, Heinzen C, Rainov NG. Alginate encapsulation of genetically engineered mammalian cells: comparison of production devices, methods and microcapsule characteristics. J Microencapsul. 2003; 20(3):303–316. [PubMed: 12881112]
21. Ohkawa K, Kitagawa T, Yamamoto H. Preparation and characterization of chitosan-gellan hybrid capsules formed by self-assembly at an aqueous solution interface. Macromol Mater Eng. 2004; 289(1):33–40.
22. Oliveira JT, Santos TC, Martins L, Picciochi R, Marques AP, Castro AG, Neves NM, Mano JF, Reis RL. Gellan Gum Injectable Hydrogels for Cartilage Tissue Engineering Applications: In Vitro Studies and Preliminary In Vivo Evaluation. Tissue Eng Part A. 2010; 16(1):343–353. [PubMed: 19702512]
23. Agnihotri SA, Jawalkar SS, Aminabhavi TM. Controlled release of cephalexin through gellan gum beads: Effect of formulation parameters on entrapment efficiency, size, and drug release. Eur J Pharm Biopharm. 2006; 63(3):249–261. [PubMed: 16621483]
24. Maiti S, Ranjit S, Mondol R, Ray S, Sa B. Al(+3) ion cross-linked and acetalated gellan hydrogel network beads for prolonged release of glipizide. Carbohydr Polym. 2011; 85(1):164–172.
25. Moslemy P, Neufeld RJ, Guiot SR. Biodegradation of gasoline by gellan gum-encapsulated bacterial cells. Biotechnol Bioeng. 2002; 80(2):175–184. [PubMed: 12209773]
26. Soonshiong P, Heintz RE, Merideth N, Yao QX, Yao ZW, Zheng TL, Murphy M, Moloney MK, Schmehl M, Harris M, et al. INSULIN INDEPENDENCE IN A TYPE-DIABETIC PATIENT AFTER ENCAPSULATED ISLET TRANSPLANTATION. Lancet. 1994; 343(8903):950–951. [PubMed: 7909011]
27. Hasse C, Klock G, Schlosser A, Zimmermann U, Rothmund M. Parathyroid allotransplantation without immunosuppression. Lancet. 1997; 350(9087):1296–1297. [PubMed: 9357413]
28. Landfester K, Musyanovych A, Mailander V. From Polymeric Particles to Multifunctional Nanocapsules for Biomedical Applications Using the Miniemulsion Process. J Polym Sci, Part A: Polym Chem. 2010; 48(3):493–515.
29. De Koker S, Lambrecht BN, Willart MA, van Kooyk Y, Grooten J, Vervaet C, Remon JP, De Geest BG. Designing polymeric particles for antigen delivery. Chem Soc Rev. 2011; 40(1):320–339. [PubMed: 21060941]
30. Lensen D, Vriezema DM, van Hest JCM. Polymeric Microcapsules for Synthetic Applications. Macromol Biosci. 2008; 8(11):991–1005. [PubMed: 18655033]
31. De Cock LJ, De Koker S, De Geest BG, Grooten J, Vervaet C, Remon JP, Sukhorukov GB, Antipina MN. Polymeric Multilayer Capsules in Drug Delivery. Angew Chem-Int Edit. 2010; 49(39):6954–6973.
32. Roh IJ, Kwon IC. Fabrication of a pure porous chitosan bead matrix: influences of phase separation on the microstructure. J Biomater Sci-Polym Ed. 2002; 13(7):769–782. [PubMed: 12296443]
33. Zhang YJ, Wei Q, Yi CB, Hu CY, Zhao WF, Zhao CS. Preparation of Polyethersulfone-Alginate Microcapsules for Controlled Release. J Appl Polym Sci. 2009; 111(2):651–657.

34. Calafiore R. Alginate microcapsules for pancreatic islet cell graft immunoprotection: struggle and progress towards the final cure for type 1 diabetes mellitus. Expert Opin Biol Ther. 2003; 3(2): 201–205. [PubMed: 12662135]

35. Kedzierewicz F, Lombry C, Rios R, Hoffman M, Maincent P. Effect of the formulation on the in-vitro release of propranolol from gellan beads. Int J Pharm. 1999; 178(1):129–136. [PubMed: 10205633]

36. Uludag H, Horvath V, Black JP, MV S. Viability and Protein Secretion from Human Hepatoma (HepG2) Cells Encapsulated in 400-pm Polyacrylate Microcapsules by Submerged Nozzle-Liquid Jet Extrusion. Biotechnol Bioeng. 1994; 44:1199–1204. [PubMed: 18618546]

37. Coutinho DF, Sant SV, Shin H, Oliveira JT, Gomes ME, Neves NM, Khademhosseini A, Reis RL. Modified Gellan Gum hydrogels with tunable physical and mechanical properties. Biomaterials. 2010; 31(29):7494–7502. [PubMed: 20663552]

38. Oliveira JT, Martins L, Picciochi R, Malafaya IB, Sousa RA, Neves NM, Mano JF, Reis RL. Gellan gum: A new biomaterial for cartilage tissue engineering applications. J Biomed Mater Res Part A. 2010; 93A(3):852–863.

39. Payne R, Yaszemski M, Yasko A, Mikos A. Development of an injectable, in situ crosslinkable, degradable polymeric carrier for osteogenic cell populations. Part 1. Encapsulation of marrow stromal osteoblasts in surface crosslinked gelatin microparticles. Biomaterials. 2002; 23(22):4359–4371. [PubMed: 12219826]

40. Oliveira JT, Gardel L, Martins L, Rada T, Gomes ME, Reis RL. Injectable gellan gum hydrogels with autologous cells for the treatment of rabbit articular cartilage defects. J Orthop Res. 2010; 28(9):1193–1199. [PubMed: 20187118]

41. Wang W, Liu XD, Xie YB, Zhang H, Yu WT, Xiong Y, Xie WY, Ma XJ. Microencapsulation using natural polysaccharides for drug delivery and cell implantation. J Mater Chem. 2006; 16(32):3252–3267.

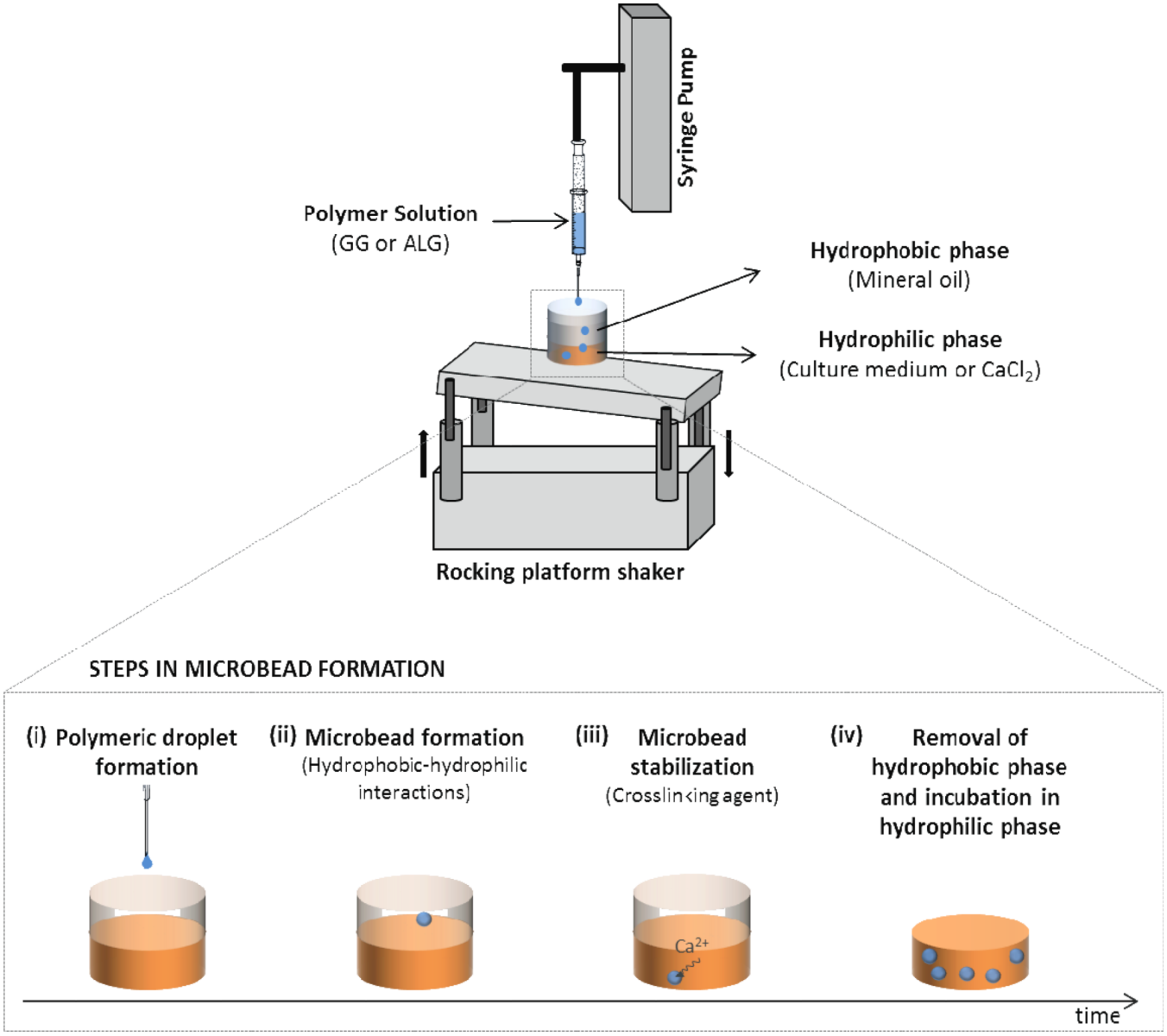

Figure 1.

Schematics of the system and of the procedure for microbead formation. Once the syringe pump starts flowing the polymer solution through the needle, a polymeric droplet is formed (i). By gravity forces, the polymeric droplet is pulled down. The rocking platform shaker allows the hydrophobic solution to repeatedly meet the polymeric droplet. When the forces of gravity and surface tension between the polymer and mineral oil (present by the action of the rocking platform) supersede the force of surface tension between the polymer and the needle, the polymer droplet falls into the hydrophobic solution. Once it drops in the hydrophobic phase, a microbead is formed through hydrophobic-hydrophilic interactions (ii). As the microbead passes the hydrophobic-hydrophilic interface, it stabilizes with the Ca^{2+} ions (iii). The resulting microbeads can be incubated in the hydrophilic phase after removing the hydrophobic solution.

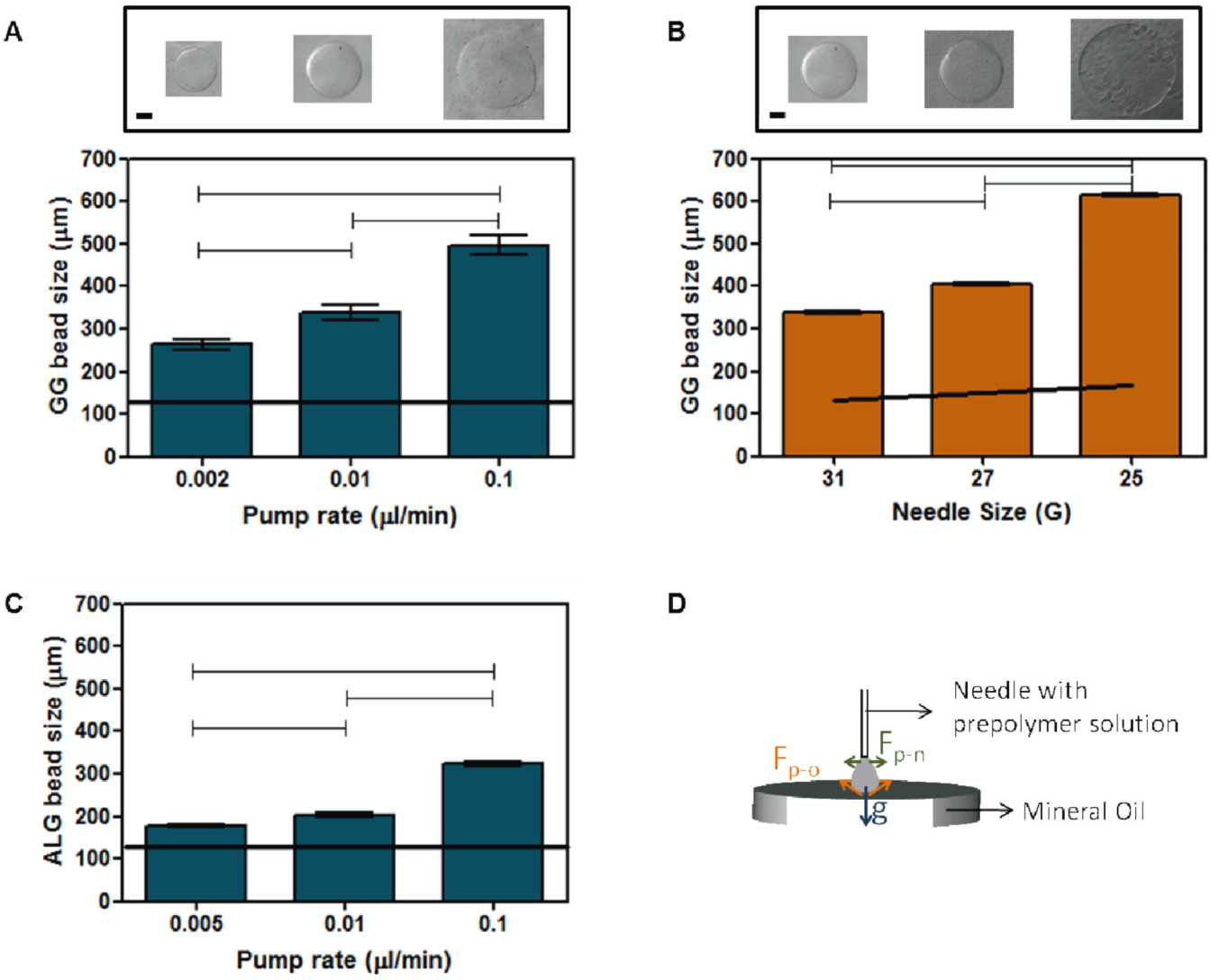

Figure 2.

Influence of system parameters over bead size of GG: (A) Pump rate (µL/min) and (B) needle size (G) ($p<0.05$). Scale bar of the microbeads is 100 µm. (C) Influence of pump rate over the microbead size using ALG ($p<0.05$). Black line corresponds to the inner diameter of the needle (µm). (D) Schematics of the action of the forces proposed to be involved on the formation of the microbeads in the hydrophobic phase: gravity (g), surface tension between the polymer and needle (F_{p-n}) and surface tension between the polymer and mineral oil (F_{p-o}) (n=30).

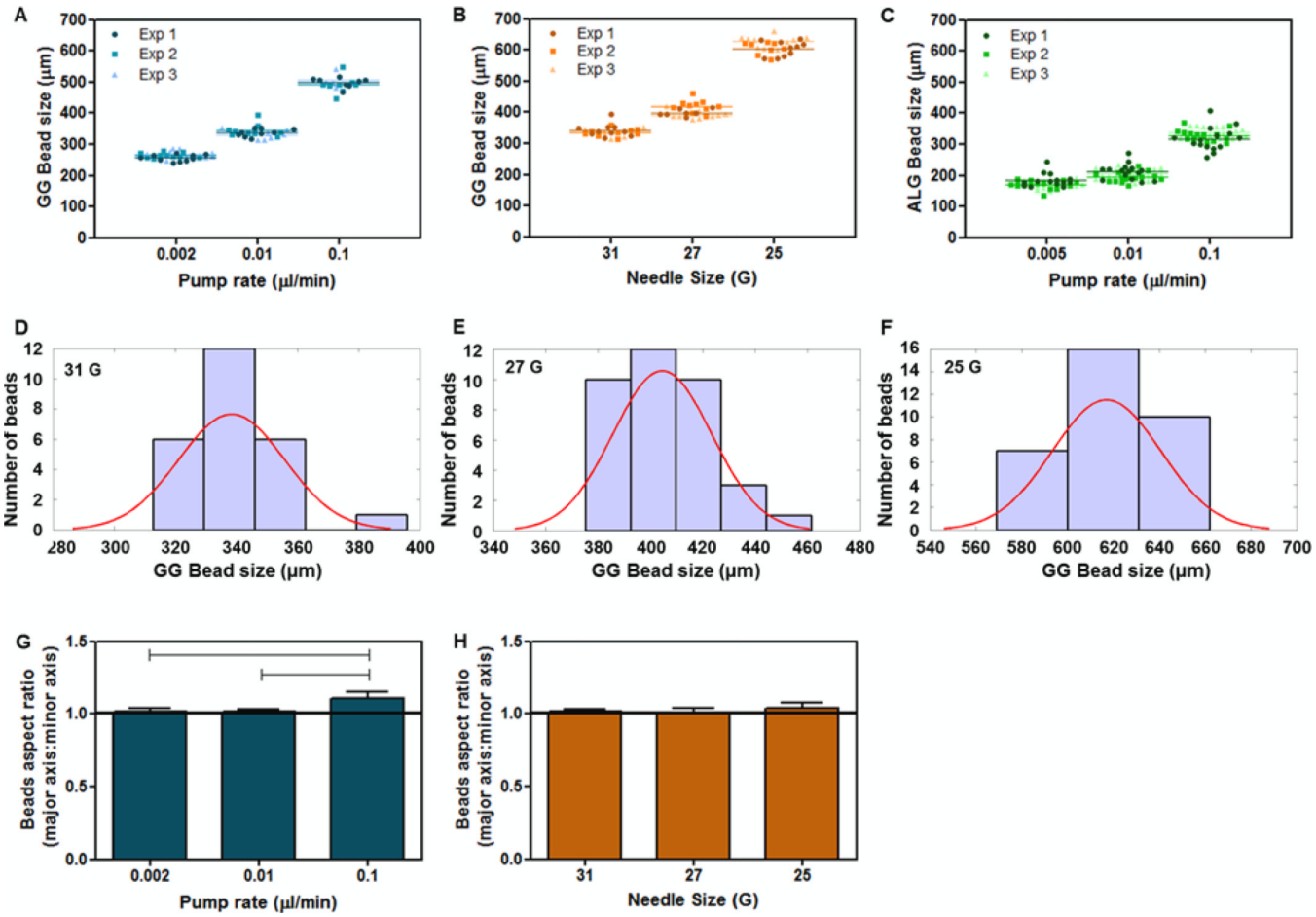

Figure 3.

Reproducibility of the system by evaluating the bead size uniformity at different (A) pump rates and (B) needle sizes for GG and for different (C) pump rates for ALG. Histogram of the distribution of GG bead size for different needle sizes: (D) 31G, (E) 27G and (F) 25G. Aspect ratio of GG microbeads at different (G) pump rates and (H) needle sizes ($p<0.05$).

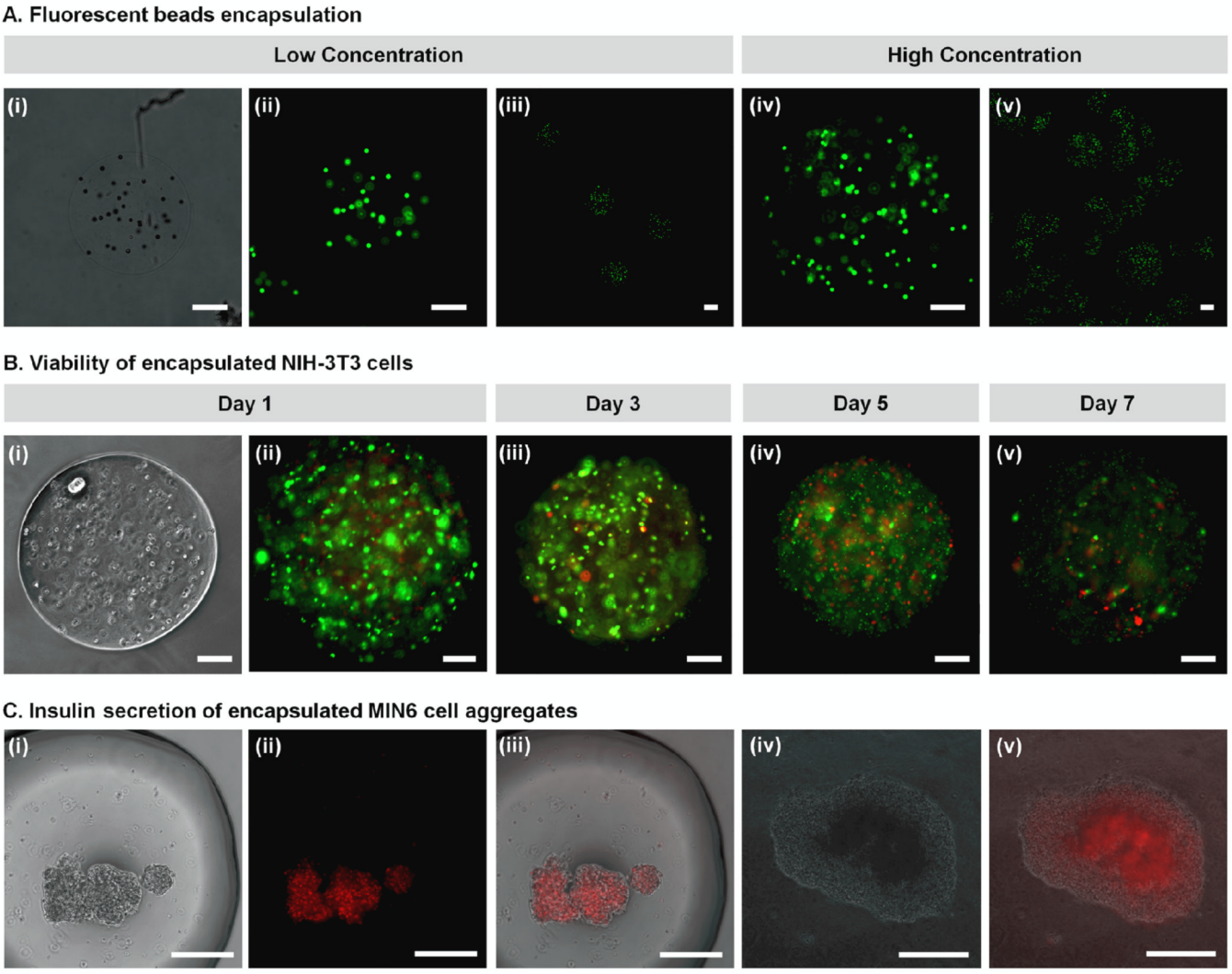

Figure 4.

Potential biological entities encapsulated with the proposed system: (A) fluorescent green microbead encapsulation in GG with two concentrations: (i,ii,iii) low, and (iv, v) high. (B) Viability (live/dead) of encapsulated NIH-3T3 cells in GG after: (i,ii) 1 day, (iii) 3 days, (iv) 5 days, and (v) 7 days in culture. (C) Insulin expression for testing the functionality of encapsulated cell aggregates in GG using antibody staining (red): (i,iv – phase images; ii – fluorescent images; iii,v – fluorescent images superimposed on the phase images). Scale bar: 100 μm.